Development and Investigation of Finite Energy Spread and Improved Emittance Relativistic Electron Beams

J. Fink, H.-B. Schilling, U. Schumacher

IPP O/41

July 1979

MAX-PLANCK-INSTITUT FÜR PLASMAPHYSIK

8046 GARCHING BEI MÜNCHEN

MAX-PLANCK-INSTITUT FÜR PLASMAPHYSIK

GARCHING BEI MÜNCHEN

Development and Investigation of Finite Energy Spread and Improved Emittance Relativistic Electron Beams

J. Fink, H.-B. Schilling, U. Schumacher

IPP O/41 July 1979

Die nachstehende Arbeit wurde im Rahmen des Vertrages zwischen dem Max-Planck-Institut für Plasmaphysik und der Europäischen Atomgemeinschaft über die Zusammenarbeit auf dem Gebiete der Plasmaphysik durchgeführt.

IPP O/41

J. Fink,
H.-B. Schilling,
U. Schumacher

Development and Investigation of Finite Energy Spread and Improved Emittance Relativistic Electron Beams

Abstract

The experiments with a divided cathode in an electron beam gun, one half of which is connected via a resistor with the high voltage terminal, lead to the generation of a low emittance electron beam with instantaneously two different energies which is suitable for suppression of collective instabilities in an electron ring accelerator. The energy difference can be varied up to 100 keV proportional to the resistance, and the sub-currents are equal. The beam parts are well separated and focussed at the injection area of the compressor, and their radial distance is about equal to the radial difference of the corresponding closed orbits, such that electron ring formation with minimum radial betatron oscillations should be possible.

I. Introduction

One of the attractive methods of ion acceleration, the electron ring accelerator (ERA), makes use of the collective fields of a ring of relativistic electrons [1,2]. The collective fields, on the other hand, impose the limitations on the attainable ring holding power (and thus the energy gain per length) of this acceleration method, mainly by collective instabilities. Most of these collective instabilities can be suppressed by Landau damping of the electrons with an instantaneous finite energy spread. As an example we mention that the threshold value N_e of the electron number in the ring, above which the negative mass instability occurs, depends quadratically on the relative energy spread $\Delta E/E$ of the electrons [2,3]. Up to this maximum electron number N_e the effect of the electromagnetic bunching forces on the ring are compensated by the dispersing action (Landau damping, produced by the energy spread $\Delta E/E$).

In previous electron ring experiments the finite electron energy spread was produced by passing the electron beam (prior to ring formation) through non-uniform energy absorbers, e.g. thin polyethylene foils of pyramidal or strip structure (saw-tooth thickness profiles) [4,5,6]. The energy absorption, however, is inherently related to an angular broadening and thus an emittance increase of the electron beam [5], which results in a reduction of the obtainable holding power.

A controllable energy spread of the beam electrons can also be produced by using separate cathode elements resistively coupled to the high-voltage terminal, as proposed by the Karlsruhe ERA group [7,8] by which method the energy spreading is not necessarily connected with an emittance increase. The Garching work to develop an electron beam source with a finite energy spread uses this principle. The cathode elements in our experimental device, however, are not arranged coaxially but in a row. This allows the electrons after their passage through the beam transport system to be injected approximately on their closed orbits

in order to minimize their radial betatron oscillations: The relative radial difference of the closed orbits of two electrons with an energy difference of ΔE is

$$\frac{\Delta R}{R} = \frac{\Delta E}{E} \cdot \frac{1}{1-n} \quad ,$$

where $$n = - \frac{R}{B_z} \frac{\partial B_z}{\partial R}$$

is the magnetic field index in the injection area. For $n = 0.4$ and $\Delta E/E = 0.05$ we get $\Delta R/R = 0.0833$. At a mean radius of $R = 18$ cm the beam center separation hence would be $\Delta R = 1.5$ cm. This is about the distance of different emitting elements in the cathode.

II. Experimental Devices

The experiments were performed with the electron beam generator Febetron 705. In a first series of experiments a modified beam tube was used that enabled easier diagnostics of voltages and currents: The 0.5 MV unit of the gun that generates the two electron beams with different energies was brought in the Febetron device from the high voltage terminal (-2 MV) to ground level at its lower potential side, and the electron beam in the remaining section was simulated by a resistor connecting the unit to the -2 MV terminal. By this method the magnitude and the time behaviour of the current are unchanged. It is, however, possible to measure the voltages at the different cathode elements. A schematic of this experimental device is given in Fig.1.

Although it was intended to split the cathode into several parts in order to obtain several sub-currents with different energies each, we started the investigation with the experimental device schematically drawn in Fig.1. The cathode is split in two halves, which can be separately placed at different distances (d and $d-\Delta d$, respectively) from the anode grid. One of them is connected via the resistor R to the high-voltage terminal.

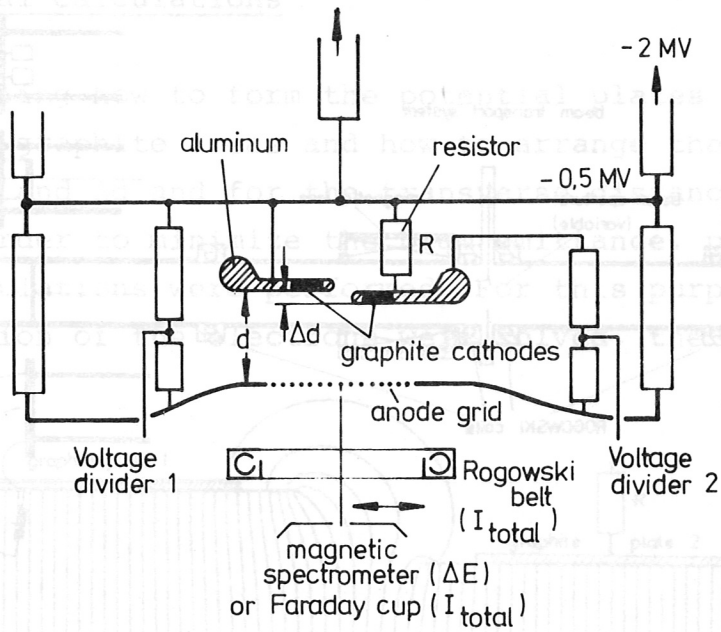

Fig.1: Schematic of the experimental device

This experimental arrangement allows the measurement of the potential difference of the two cathode halves (from the difference signal of the voltage dividers) and hence the deduction of the electron energy difference ΔE. With the resistance value R the current I_2 emitted from the (right) cathode half at the distance d-Δd is obtained. The total current I_{total} is measured with a Rogowski coil downstream from the anode grid, and independently by the Faraday cup measurement. An arrangement of Faraday cups side by side even makes it possible to determine the relevant sub-currents. The magnetic spectrometer allows to verify the electron energy distribution as obtained from the voltage measurements.

The second series of experiments was devoted to measurements of the beam current, its density and energy distribution in the device as to be applied at the PUSTAREX experiment [9]. Fig.2 shows schematically the arrangement in which the cathode-grid device of Fig.1 is transferred to the high voltage terminal (-2 MV) of the Febetron, only the voltage dividers being removed. The other potential plates of the gun are those of ref.10.

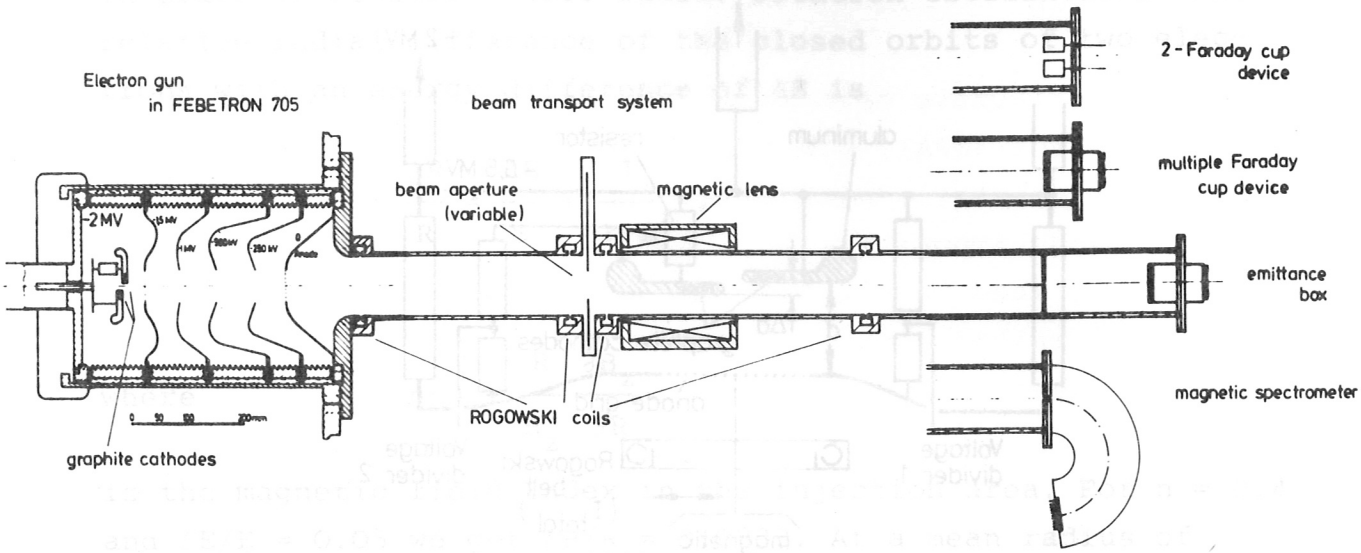

Fig.2: Schematic of the electron gun arrangement with beam transport system and diagnostics

The gun is connected to the beam transport system, and the beam is focussed by a single magnetic lens. The beam parameters at the end of the transport system, where the electrons enter the compressor magnetic field, are measured by an array of Faraday cups (see ref.11) to determine the electron current density and by a magnetic spectrometer to find the electron energy distribution. The cup array together with a small aperture, moreover, serves to measure the electron beam emittance.

The electron beam development with these devices aimes to obtain an electron beam of finite energy spread and an emittance as small as possible. To attain a small emittance not only the acceleration field (including the selffield effects) has to be homogeneous, the emitting areas also have to be smooth. Hence the needle structure of the cathode - as used in previous experiments - is not advantageous, and we decided to apply plane graphite plates [12] as emitting areas (see Fig.1). In order to avoid enhanced electron emission at the plate edges, the graphite plate units are surrounded by conducting surfaces which shape the electric field distribution.

III. Numerical Calculations

To get a feeling how to form the potential plates surrounding the emitting graphite areas and how to arrange them (optimum values for d and Δd and for the transverse distance of the two plates) in order to minimize the beam emittance, particle trajectory calculations were performed. For this purpose the equations of motion of the electrons were solved, the fields being

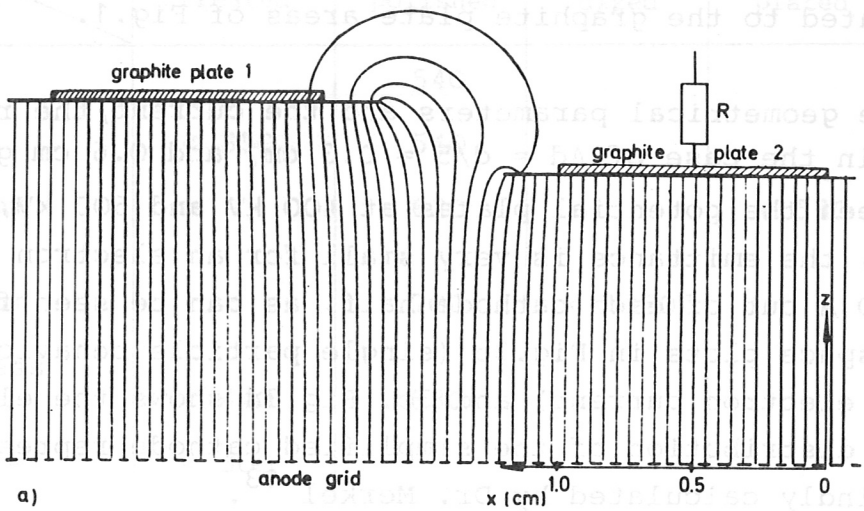

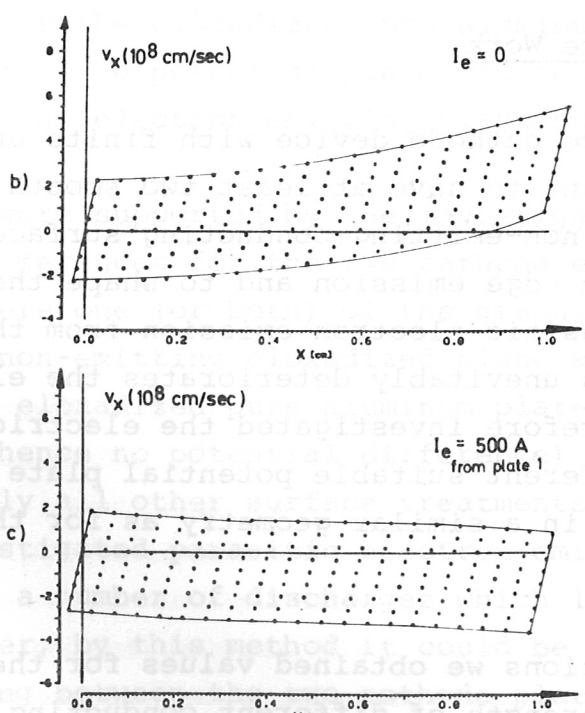

Fig.3: Electric field distribution (a) and phase space areas at anode grid (for plate 1) without (b) and with (c) electron current for the two element cathode

composed of the external electric field and the electric and magnetic fields generated by the beams and their images. In order to get a treatable representation of the electric field, the cathode structure of Fig.1 was simplified to be represented by two semi-infinite planes with a certain gap width and at distances d and d-Δd, respectively, from an infinite plane at ground potential. It was furthermore assumed that the electron emission occurred only from limited areas on both potential plates related to the graphite plate areas of Fig.1.

Varying the geometrical parameters and the current, the results[13] show that in the case of $\Delta d = d/5 = 0.3$ cm, and 0.6 cm gap width between the potential plates at 400 kV and 500 kV, respectively, the emittance is very small for an electron current of 500 A out of each cathode half, as can be seen from the phase space plots in Fig.3b (single particle behaviour or negligible electron current) and 3c. Fig.3a shows the electric field line distribution of the simplified cathode representation, as kindly calculated by Dr. Merkel [13].

IV. Cathode Surface Work

For a low emittance cathode device with finite energy spread it is very important to have at least two smooth emitting areas inserted in non-emitting conducting surfaces in order to avoid unfavourable edge emission and to shape the potential distribution. Parasitic electron emission from the surrounding potential surfaces unevitably deteriorates the electron beam emittance. We therefore investigated the electrical breakdown properties of different suitable potential plate materials for pulse discharging in a similar geometry as for the cathode device of Fig.1.

Under these conditions we obtained values for the electrical breakdown field strength of different conducting materials for some different surface treatment as given in table 1.

Table 1

Electrical breakdown field strength E [kV/cm] of different potential plate materials and coatings at pulse discharges as in the electron gun

Material \ Surface treatment	un-treated	electrically polished	eloxadized	nickel-plated	Kapton coated
Copper		540			730
Brass	< 350	540			860
Aluminum		620		< 530	860
Pure aluminum		700	< 1350		
Stainless steel	< 440	580			830
Graphite	< 300				

It turns out that the eloxadized pure aluminum surfaces are most suitable for the potential plates in connection with the graphite plates as electron emitting plane surfaces.

These results were supported by the investigation of currents and voltage differences for the two cathode elements in Fig.1 in the case where one (or both) of the graphite elements was replaced by a non-emitting eloxadized plane aluminum plate. In the case of eloxadized pure aluminum plates no electron emission (and hence no potential difference) was observed, while for nearly all other surface treatments and all other materials investigated parasitic electron emission occurred at least after a number of discharges which led to surface damage. Moreover, by this method it could be proven that no short-circuiting between the two cathode plates occurred up to the highest desired potential differences (about 100 kV).

V. Results from the Model Experiment

The experiments with the model device (Fig.1) mainly concentrated on the choice of the structure and material of the cathode elements and the surrounding plates. Furthermore, great effort was expended to find the optimum values for the mechanical parameters of the two cathode halves (size of the emitting areas, gap width and distances d and Δd) as a function of the resistor R. Some experimental results are shown in Figures 4 to 7. The dependence of the total electron current $I_{total} = I_1 + I_2$ and of the partial current I_2 (from the cathode half with the resistor) is plotted versus the resistance R in Fig.4.

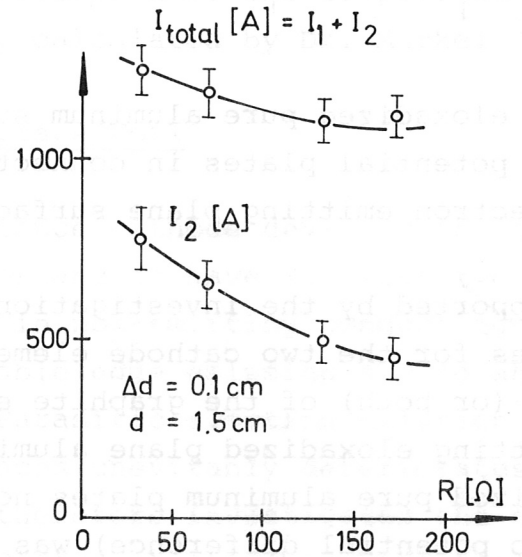

Fig.4: Total current I_{total} and partial current I_2 versus the resistance R for fixed distances Δd and d

It turns out that at fixed distances Δd and d the partial current I_2 strongly drops with increasing R, while I_{total} only slightly goes down. How sensitive I_2 is to variations of Δd might be seen from Fig.5, where I_2 is plotted versus the distance Δd of both cathode elements, normalized to d and to the resistance R. The data points - the same resistance values R are indicated by the same symbols - can be roughly represented by one curve. The current I_2 reaches about half the total current for $\Delta d/(R \cdot d) \approx 10^{-3} \Omega^{-1}$. This corresponds to cathode spacings such that the mean electric field strengths in both diode halves (see Fig.3a) is just about equal, in which case the beam emittance is expected to be minimum.

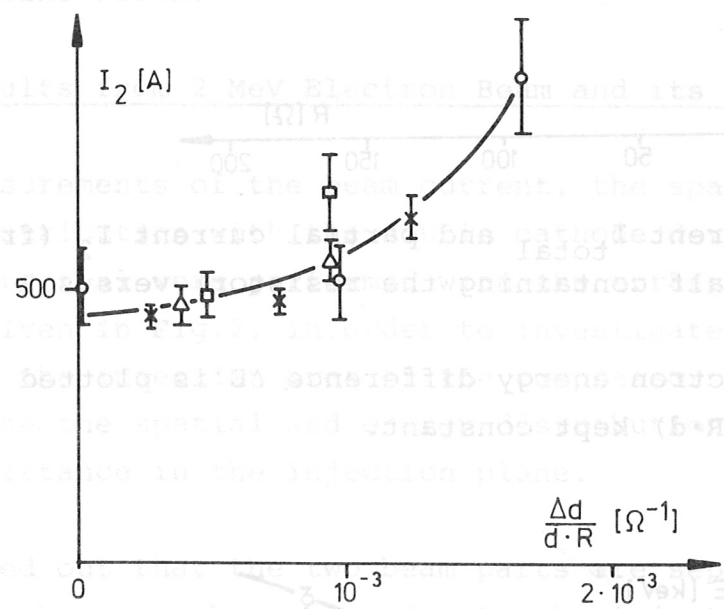

Fig.5: Partial current I_2 versus normalized cathode distance

We now plot in Fig.6 the total current I_{total} and the partial current I_2 versus R for fixed cathode distances, such that $\Delta d/(R \cdot d) \approx 10^{-3} \Omega^{-1}$ and hence both cathode halves have approximately equal field strengths. Both currents are nearly independent of R, and both cathode halves emit about equal currents, i.e. I_2 is about half the value of I_{total}. This goal is already reached with equal size of both graphite cathode plates.

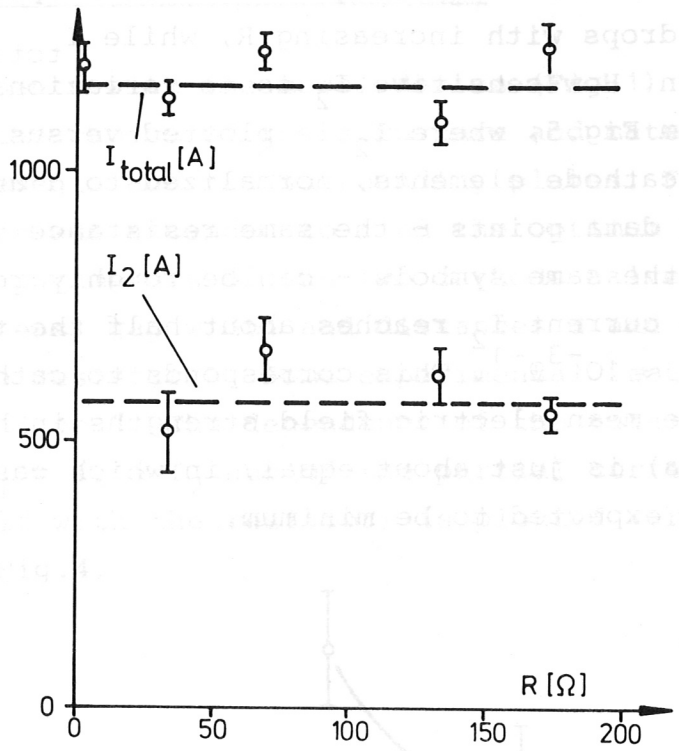

Fig.6: Total current I_{total} and partial current I_2 (from the cathode half containing the resistor) versus R

In Fig.7 the electron energy difference ΔE is plotted versus R, also for $\Delta d/(R \cdot d)$ kept constant.

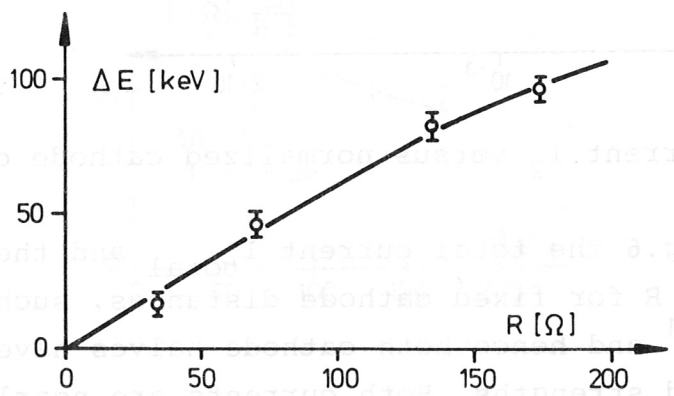

Fig.7: The electron energy difference versus the resistance R

The energy difference ΔE increases about linearly with R (at a slope of 0.6 keV/Ω) and reaches a value of ΔE = 100 keV with about R = 170 Ω, which corresponds to the desired relative energy difference of $\Delta E/E \approx 5\%$ at 2 MeV maximum electron energy. The values of the energy difference were obtained from the difference of the voltage divider signals. They could be verified by the magnetic spectrometer results (although these were very sensitive to the temporal energy changes). The electron energy distribution resembled - more or less - two monoenergetic peaks at a distance of ΔE. The resolution of the magnetic spectrometer (although being $\delta E/E < 0.008$ or $\delta E < 4$ keV) was not sufficient to show a finite line width.

VI. Results from 2 MeV Electron Beam and its Transport

The measurements of the beam current, the spatial and the energy distribution with the double cathode device at full Febetron potential were performed with the arrangement schematically given in Fig.2, in order to investigate the beam transport to the injection area of the compressor device and to determine the spatial and energy distribution as well as the beam emittance in the injection plane.

It turned out that the two beam parts are separated in space and that both can be focussed into the injection plane as has been calculated by W. Dommaschk [14]. By a corresponding rotation of the cathode mounting support it was easily possible to focus the partial beams such that the electrons with the higher energy can be injected at the larger radius and correspondingly those with the smaller energy at a smaller radius. Moreover, it was possible to make the radial beam center distance nearly equal to the radial difference (about 1.2 cm) of the closed orbits for the electrons with ΔE energy difference, since $\Delta R = R \cdot \Delta E/E \cdot (1-n)^{-1} \approx 1.2$ cm for R = 18 cm, n = 0.4 and $\Delta E/E = 0.04$.

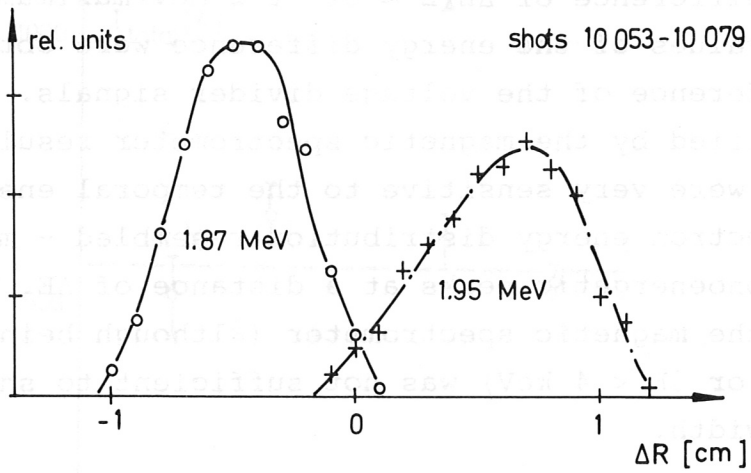

Fig.8: Relative beam current density versus radius for the two electron energies

An example as obtained from the magnetic spectrometer measurements is given in Fig.8. One easily concludes that the locations for the current distributions of the two electron beams with different energies are nearly completely separated and that the current in both beam parts - as obtained by radial integration - is about equal, although the shapes are slightly different. The maxima are separated by about 1.2 cm. The absolute value of the current density is about 800 A/cm^2 maximum.

The spatial electron beam current density was measured by the array of Faraday cups [11]. Fig.9 gives an example of the current density obtained from one shot with about 100 Faraday cups. Although the spatial resolution is limited, two clearly separated maxima with the desired energy difference of 4 to 5% can be seen. The values of the outer regions are exaggerated compared to the instantaneous current density distribution due to the time integration as was verified by time resolved measurements.

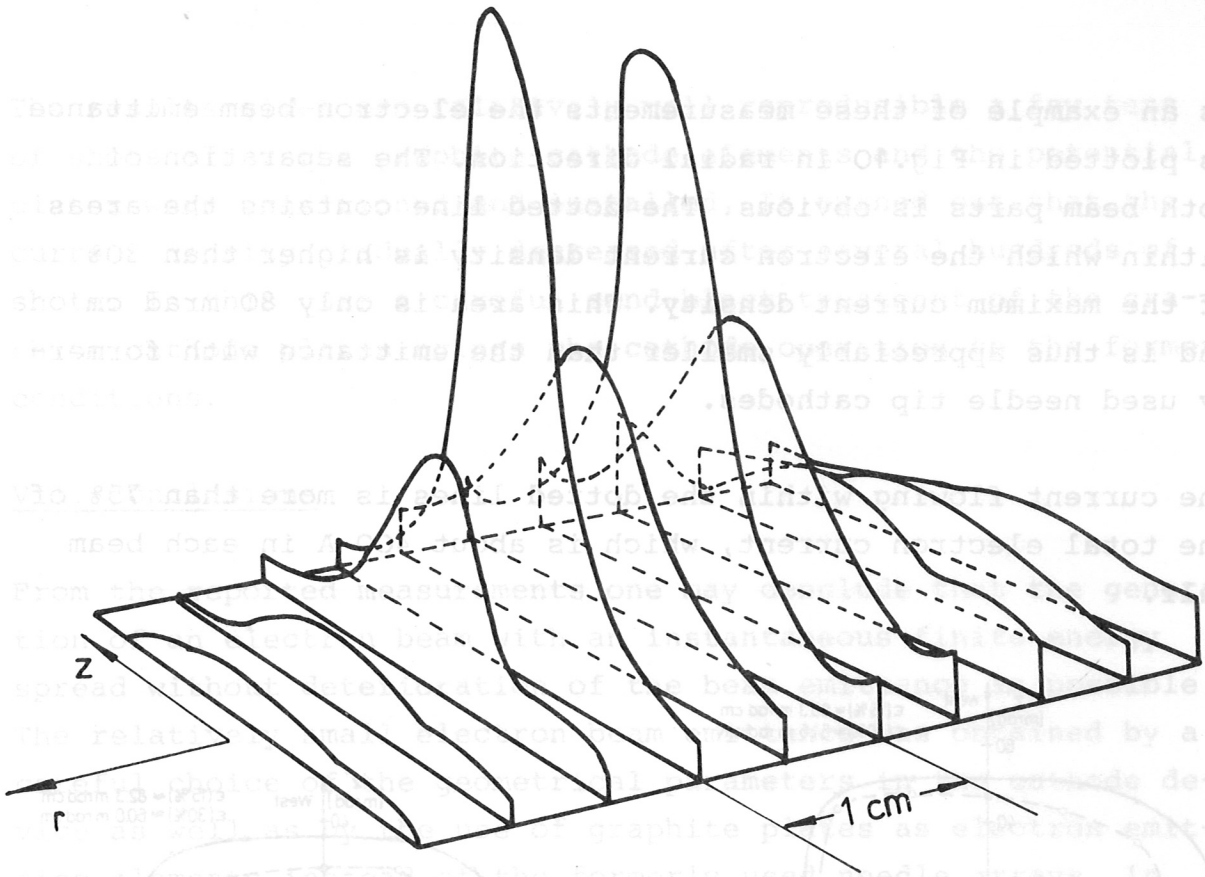

Fig.9: Relative current density (time integrated) as obtained from the multiple Faraday cup device

The electron beam emittance is obtained with the same multiple Faraday cup device about 25 cm downstream behind a small aperture, all being movable perpendicular to the beam axis in order to scan the beam.

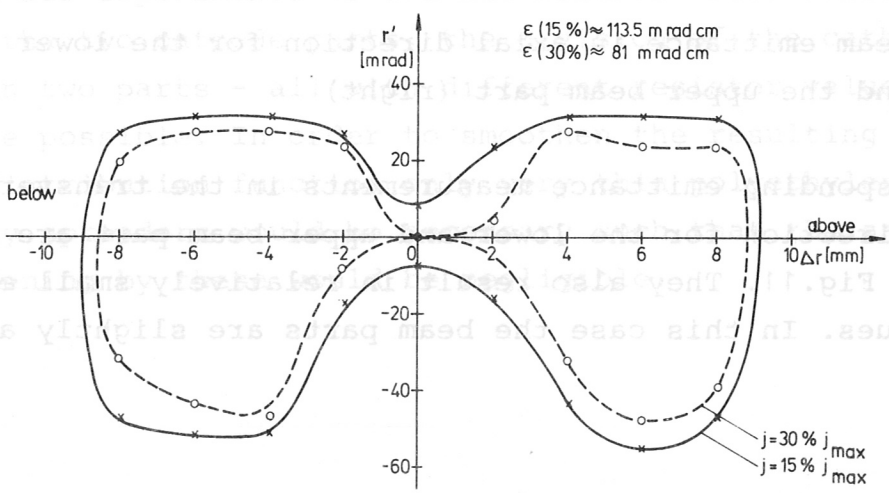

Fig.10: Beam emittance in radial direction

As an example of these measurements the electron beam emittance is plotted in Fig.10 in radial direction. The separation of both beam parts is obvious. The dotted line contains the areas within which the electron current density is higher than 30% of the maximum current density. This area is only 80 mrad cm and is thus appreciably smaller than the emittance with formerly used needle tip cathodes.

The current flowing within the dotted lines is more than 75% of the total electron current, which is about 400 A in each beam half.

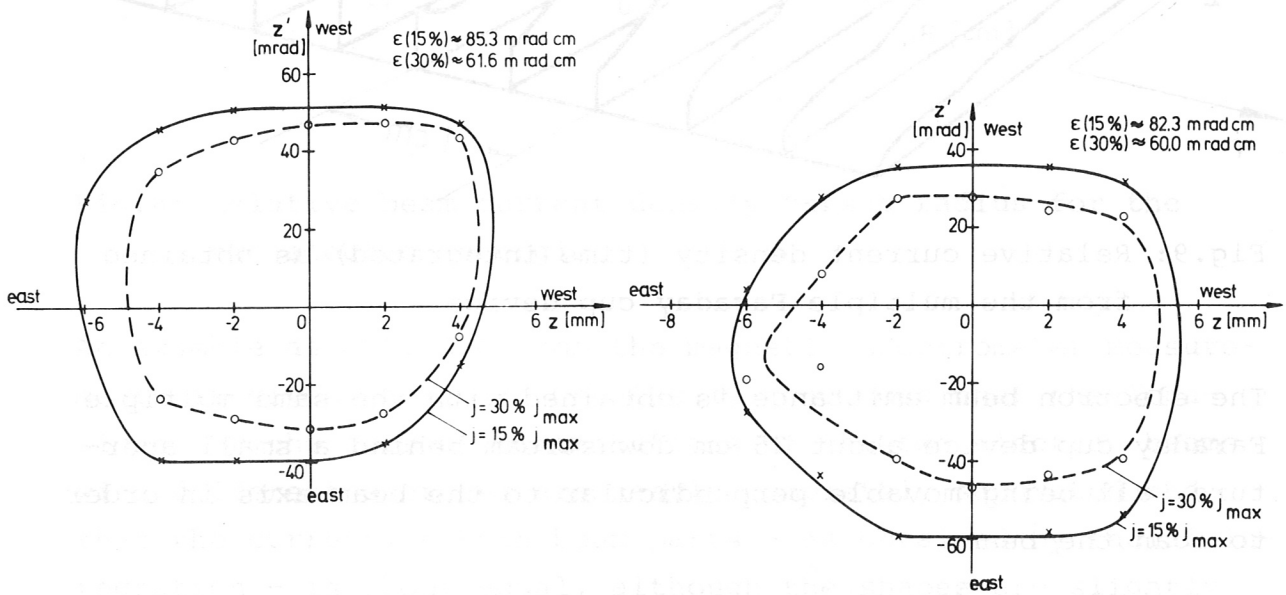

Fig.11: Beam emittance in axial direction for the lower (left) and the upper beam part (right)

The corresponding emittance measurements in the transverse (axial) direction for the lower and upper beam part are represented in Fig.11. They also result in relatively small emittance values. In this case the beam parts are slightly approaching.

The results given are relatively well reproducible a few tens of shots after the graphite cathode elements and the potential plates were conditioned and installed. It turned out that the current density gradually decreased after several hundreds of shots. In this case a careful sand-blast treatment of the graphite cathode plates brings the cathode operation to the former conditions.

VII. Conclusions

From the reported measurements one may conclude that the generation of an electron beam with an instantaneous finite energy spread without deterioration of the beam emittance is possible. The relatively small electron beam emittance was obtained by a careful choice of the geometrical parameters in the cathode device as well as by the use of graphite plates as electron emitting elements instead of the formerly used needle arrays. In our experiments, however, only a double humped energy distribution was produced, although for negative mass instability suppression a smooth distribution would be desirable. This can be obtained by the insertion of a small polyethylene foil of sawtooth thickness profile into the beam path at the end of the transport system, as is done in the last experimental runs of PUSTAREX.

Since in our experiments we did not observe short-circuiting between the two cathode parts, the division of the cathode into more than two parts - all with different resistor values - should be possible. In order to smoothen the resulting multihumped distribution function only very thin polyethylene foils as energy spreaders would be necessary such that the angular beam widening by these would be negligible.

Acknowledgements

The authors express their gratitude to Dr. W. Dommaschk for fruitful discussions about beam transport calculations, to Dr. P. Merkel for kindly calculating the electric field distribution of the diode, and to E. Springmann for skilfully carrying out the particle trajectory calculations. Several discussions and the interest of them and of Dr. C. Andelfinger, Dr. W. Herrmann, Prof. A. Schlüter and M. Ulrich are gratefully acknowledged.

References

1 V.I. Veksler, V.P. Sarantsev, A.G. Bonch-Osmolovskii, G.I. Dolbilov, G.A. Ivanov, I.N. Ivanov, M.L. Iovnovich, I.V. Koshkunov, A.B. Kuznetsov, V.G. Mahankov, E.A. Perelshtein, V.P. Rashevskii, K.A. Reshetnikova, N.B. Rubin, S.B. Rubin, P.I. Ryltsev, O.I. Yarkovoi: Atomnaya Energiya 24, 317 (1968); Proc.6th Int.Conf.on High-Energy Accelerators, Cambridge, Mass., USA (1967) (Cambridge Electron Accelerator Report No.CEAL-2000, 1967), p.289; Report JINR-P-3440-2, Dubna (USSR), 1967

2 U. Schumacher: Springer Tracts in Modern Physics 84 (1979)

3 E. Keil, W. Schnell: CERN Internal Report ISR-TH-RF-69-48, CERN, Geneva (1969)

4 A. Faltens, G.R. Lambertson, J.M. Peterson, J.B. Rechen: Proc.9th Int.Conf.on High Energy Accelerators, SLAC, Stanford/USA, 1974, p.226

5 J. Fink, W. Ott: MPI für Plasmaphysik, Garching, Report IPP O/17 (July 1973)

6 U. Schumacher, M. Ulrich: Proc.II.Symp.on Coll.Methods of Acceleration, Dubna 1976, p.38

7 C.H. Dustmann, W. Heinz, H. Krauth, L. Steinbock, W. Zernial: Proc.9th Int.Conf.on High Energy Accelerators, SLAC, Stanford USA, 1974, p.250

8 C.H. Dustmann: Dissertation, Universität Karlsruhe 1974

9 C. Andelfinger, E. Buchelt, W. Dommaschk, J. Fink, W. Herrmann, I. Hofmann, A. Luccio, P. Merkel, D. Jacobi, H.-B. Schilling, A. Schlüter, U. Schumacher, M. Ulrich: IEEE Transactions on Nuclear Science, Vol.NS-24, No.3, June 1977

10 C. Andelfinger, W. Ott: MPI für Plasmaphysik, Garching, Report IPP O/13 (Mai 1972)

11 H.-B. Schilling: MPI für Plasmaphysik, Garching, Report IPP O/40 (Juli 1979)

12 R.K. Parker, R.E. Anderson, C.V. Duncan: J.Appl.Physics 45, 2463 (1974)

13 The electric field calculations were kindly performed by Dr. P. Merkel.

14 W. Dommaschk: private communication